

Supporting Information

Exploring Ligand-Centered Electrocatalytic H₂O Reduction: Hydrogen Generation with a Soluble Ni(II) Octabutoxyphthalocyanine Complex

Josh Brown, Darrin Richeson*

Synthesis of Ni(II)1,4,8,11,15,18,22,25-octabutoxy-phthalocyanine

Under N₂, the ligand (purchased from Sigma-Aldrich), H₂Pc(BuO)₈, (300mg, 0.275mmol) and Ni(CH₃CO₂)₂·4H₂O (0.6890g, 2.77mmol) were dissolved in dimethylformamide. The mixture was refluxed for 4 hours and then cooled to room temperature. 80mL of cold water was added to the mixture causing green microcrystals of NiPc to crash out of solution. The crystals were filtered and washed with more water and cold ethanol with a yield of 71%. UV-vis (DCM) λ_{max}, nm (log ε): 734 (5.75). NMR (C₆D₆): 7.54 (s, 2,3,9,10,16,17,23,26-Ar H), 4.92 (t,OR-1 CH₂), 2.26 (m, OR-2 CH₂), 1.78 (m, OR-3 CH₂), 1.10 (t,OR-4 CH₃). Single crystals were obtained using slow diffusion; the complex was dissolved in DCM using pentane as the external solvent. The unit cell was confirmed to match through single crystal x-ray diffraction with the previously reported structure through the CCDC database.¹

Electrochemistry:

All cyclic voltammetry (CV) experiments were carried out under nitrogen. Samples were prepared in a glovebox and sealed before removing for measurement. CV and bulk electrolysis were performed on a VersaSTAT 3 (Princeton Applied Research) potentiostat. A conventional three-electrode system was employed. A glassy carbon electrode (diameter=0.4 cm) was used as the working electrode, a Pt wire as the counter electrode, and an Ag wire was used as a pseudo-reference electrode for CV experiments. For bulk electrolysis experiments, a glassy carbon rod (diameter=0.4 cm; length 3 cm) was used as the working electrode, a coiled Pt wire as the auxiliary electrode, and an Ag wire was used as a pseudo-reference electrode. Ferrocene was added as an internal reference after purging with N₂ and measured before and after water addition. Tetra-n-butylammonium hexafluorophosphate (TBAHFP), the supporting electrolyte, was purchased directly from Sigma-Aldrich. The electrolyte solution, 0.1 M TBAHFP in THF, was saturated with N₂ by assembling the cell in the glovebox. The concentration of catalyst was 0.5mM in each experiment. For CVs and bulk, 15 mL of THF was used. First principles of the enhancements were computed to demonstrate the inflection point as a minimum value in a similar manner to previous work.² Hydrogen production was measured using an Agilent 7820 A gas chromatograph equipped with a thermal conductivity detector (TCD) using an Agilent select permanent gases column. The amount of H₂ was determined using a calibration curve.

UV-vis Spectroscopy:

Experiments were performed on a Cary-100 instrument using a double-beam correction. Spectra were obtained in air at a concentration of approximately 0.025mM. The spectral bandwidth of the instrument is 2nm. Scans were completed at a rate of 600nm/minute with a 1nm data interval. The cuvettes used were quartz and had a 1cm pathlength.

Spectroelectrochemical analysis:

The potentiostat and spectrophotometer used for these experiments were the same as those described above. Consecutive controlled potential electrolysis experiments were set on the potentiostat at a stepped potential (-0.05V increases each time) and held for 90 seconds. 30 seconds after each potential change a UV-vis spectrum was obtained. The scans were completed from 850-350nm at a scan rate of 1000nm/minute with a 1.67nm data interval. The cell/cuvette used for these experiments was the Honeycomb UV/Vis spectroelectrochemical Cell Kit, from Pine Research. The quartz cell had a pathlength of 1.70nm. The electrochemical cell employed a 3-electrode system. The working electrode and counter electrodes were contained on a single "honeycomb electrode card." This card has a gold honeycomb shaped working electrode that is situated directly in the beam path of the spectrophotometer. The counter electrodes are located just above the working electrode component as 2 large, rectangular, gold bars. The Ag/AgCl reference electrode was placed inside the cell away from the beam path. Experiments were referenced to a blank that contained only the THF or DCM solvent and TBAHFP electrolyte.

Computational details:

Computations were performed using the Gaussian 09 software package through the WebMO interface. Initial structures were established from single crystal-XRD coordinates and intermediates were proposed by addition of single protons and electrons, assuming singlet and doublet spin states for electron additions. All computations were performed at the M06L level of theory.³ Optimization and vibrational frequencies were computed using the def2-SVP basis set. Absolute minima of the electronic structures were confirmed by verifying an absence of negative vibrational frequencies before single point energy calculations were performed.⁴⁻⁸ Molecular energy single point calculations and molecular orbital isosurface simulations were performed using the def2-TZVP basis set. Molecular orbitals were visualized using Chemissian software. UV-vis spectra and excited states were simulated at the B3LYP level of theory and def2-TZVP basis set. The polarizable continuum model (PCM) was used to simulate a solvent system of water for all optimization, molecular energy, and UV-Vis/excited state computations. During the generation of MO figures in this document, Chemissian was also used to evaluate electron density contributions, describing the proportion localized on each group. These values are portrayed as decimal, whose summation combined with other unlisted exterior ligand contributors totals a value of 1. Contributions are listed as; 'Ni center' = metal center, 'N-Ni' = Coor-N, 'N' = bi-N, and 'N-H' = protonated Coor-N.

Foot-of-the-wave analysis:

The foot-of-the-wave analysis (FOWA) allows for an estimate of the reaction rate for an electrocatalytic process that does not show the limiting S-curve behavior.^{9,10} This analysis examines the data at the earliest points in the catalytic wave, before E_{cat} . The resulting curve is then fitted to a linear function within the region that the parent function remains linear and the slope of this line can be used to extract the k_{FOW} of the electrocatalytic reaction of interest. The k_{FOW} is often presented as turnover frequency (TOF). Strictly speaking, this TOF is the number of moles of product produced per unit time per mole of catalyst contained in the reaction-diffusion layer at the electrode and not relative to the catalyst molecules in the bulk solvent. Furthermore, TOF is only equal to k_{FOW} when the applied potential has converted all the catalyst molecules into the active reduced form.

Following the FOWA method described in the literature⁹⁻¹², the first step is to use the applied potential, E , and the potential where the catalyst undergoes the reduction process, E_{redox} , in the following relationship:

$$\exp\left[\frac{nF}{RT}(E - E_{redox})\right] \quad \text{eqn. 1}$$

Where R is the universal gas constant, T is the temperature, n is the number of electrons transferred to the catalyst, and F is the Faraday constant. This relationship used in the FOWA relationship given by equation 2 using the ratio of the catalytic current (i_c) divided by the non-catalytic Faradaic peak current (i_p) of a reduction wave (E_{redox}):

$$i_c/i_p = 2.24\sqrt{\left(\frac{RT}{nFv}\right)(k_{FOW})} \frac{1}{1 + \exp\left[\frac{nF}{RT}(E - E_{redox})\right]} \quad \text{eqn. 2}$$

In this equation, v is the scan rate in V/s. Taking the ratio of i_c to i_p simplifies the overall analysis by avoiding the determination of catalyst diffusion coefficient and electrode surface area.

With this approach a plot i_c/i_p versus $\frac{1}{1 + \exp\left[\frac{nF}{RT}(E - E_{redox})\right]}$ at the “foot of the wave” allows for a linear extrapolation. The slope of this line, m , is given by equation 3.

$$m = 2.24\sqrt{\left(\frac{RT}{nFv}\right)(k_{FOW})} \quad \text{eqn. 3}$$

and

$$k_{FOW} = 0.776 (m)^2 \quad \text{eqn. 4}$$

In this set of experiments we used $n = 1$, corresponding the third reduction event with a water concentration of 1.44M, as the first rate-determining chemical step. This leads to a lower limit to TOF.

For a general multielectron catalytic system, the number of unique electron-transfer processes that occur at the electrode per catalyst (n) and the catalyst equivalents used per turnover (n') are incorporated into eqs 2 and 3, giving eqs 5 and 6.¹²

$$i_c/i_p = 2.24\sqrt{\left(\frac{RT}{nFv}\right)n'(k_{FOW})} \frac{1}{1 + \exp\left[\frac{nF}{RT}(E - E_{redox})\right]} \quad \text{eqn. 5}$$

$$m = 2.24\sqrt{\left(\frac{RT}{nFv}\right)n'(k_{FOW})} \quad \text{eqn. 6}$$

In the case of water reduction to hydrogen, $n' = 2$ and

$$k_{FOW} = 0.388(m)^2 \quad \text{eqn. 7}$$

References:

- 1 T. C. Gunaratne, A. V. Gusev, X. Peng, A. Rosa, G. Ricciardi, E. J. Baerends, C. Rizzoli, M. E. Kenney and M. A. J. Rodgers, *Journal of Physical Chemistry A*, 2005, **109**, 2078–2089.
- 2 J. Brown, J. Ovens and D. Richeson, *ChemSusChem*, , DOI:10.1002/cssc.202102542.
- 3 D. G. Gusev, *Organometallics*, 2013, **32**, 4239–4243.
- 4 C. K. Williams, G. A. McCarver, A. Chaturvedi, S. Sinha, M. Ang, K. D. Vogiatzis and J. “Jimmy” Jiang, *Chemistry - A European Journal*, , DOI:10.1002/chem.202201323.
- 5 N. Rodríguez-López, Y. Wu, Y. Ge and D. Villagrán, *Journal of Physical Chemistry C*, 2020, **124**, 10265–10271.
- 6 A. Chaturvedi, G. A. McCarver, S. Sinha, E. G. Hix, K. D. Vogiatzis and J. Jiang, *Angewandte Chemie - International Edition*, , DOI:10.1002/anie.202206325.
- 7 J. Jiang, K. L. Materna, S. Hedström, K. R. Yang, R. H. Crabtree, V. S. Batista and G. W. Brudvig, *Angewandte Chemie*, 2017, **129**, 9239–9243.
- 8 C. K. Williams, G. A. McCarver, A. Lashgari, K. D. Vogiatzis and J. J. Jiang, *Inorg Chem*, 2021, **60**, 4915–4923.
- 9 C. Costentin, M. Robert and J.-M. Savéant, *Chemical Society reviews*, 2013, **42**, 2423–36.
- 10 C. Costentin, S. Drouet, M. Robert and J. M. Savéant, *Journal of the American Chemical Society*, 2012, **134**, 11235–11242.
- 11 E. S. Rountree and J. L. Dempsey, *Journal of the American Chemical Society*, 2015, **137**, 13371–13380.
- 12 E. S. Rountree, B. D. McCarthy, T. T. Eisenhart and J. L. Dempsey, *Inorganic Chemistry*, 2014, **53**, 9983–10002.

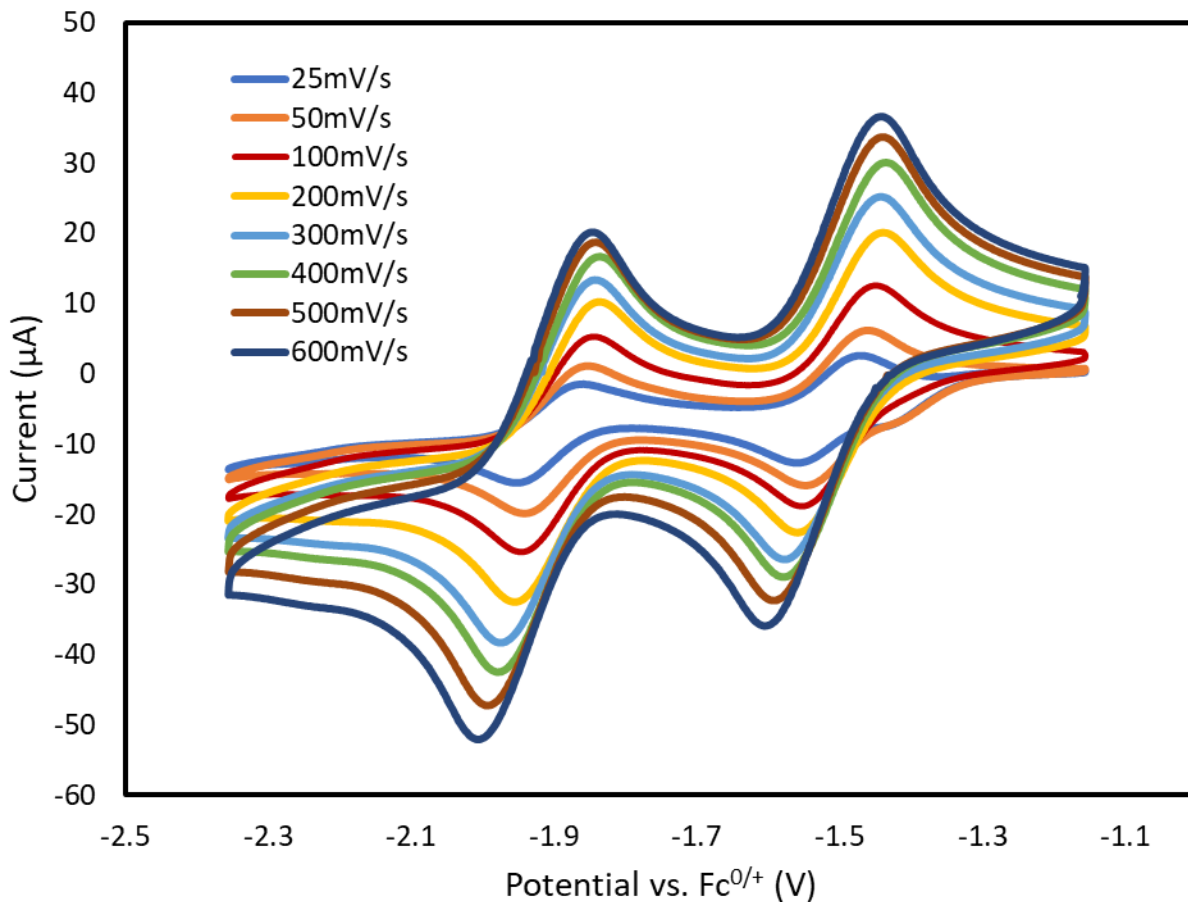


Figure S1: CV of 0.5mM NiPc in DCM scanned between -1.15V and -2.35V with a varying scan rate and electrolyte (TBAHFP) concentration of 0.1M

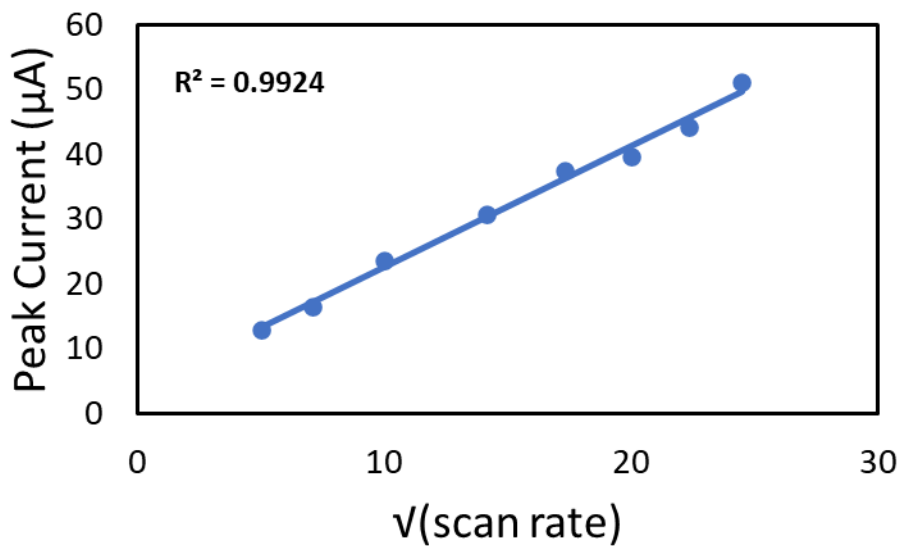


Figure S2: Plot of the reduction peak current value from figure S1 as a function of the square root of the scan rate at the first redox event (-1.55V vs $\text{Fc}/\text{Fc}^{+/0}$).

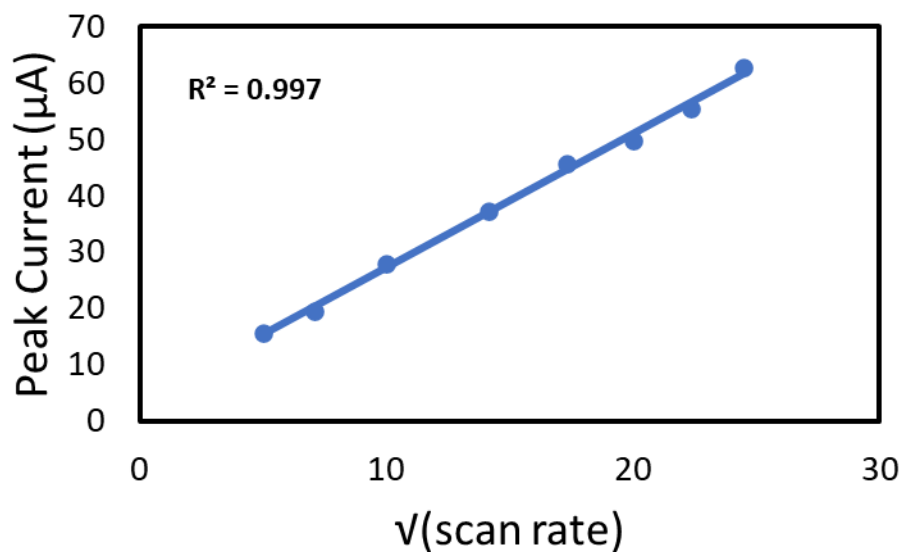


Figure S3: Plot of the reduction peak current value from figure S1 as a function of the square root of the scan rate at the second redox event (-1.95V vs $\text{Fc}/\text{Fc}^{0/+}$).

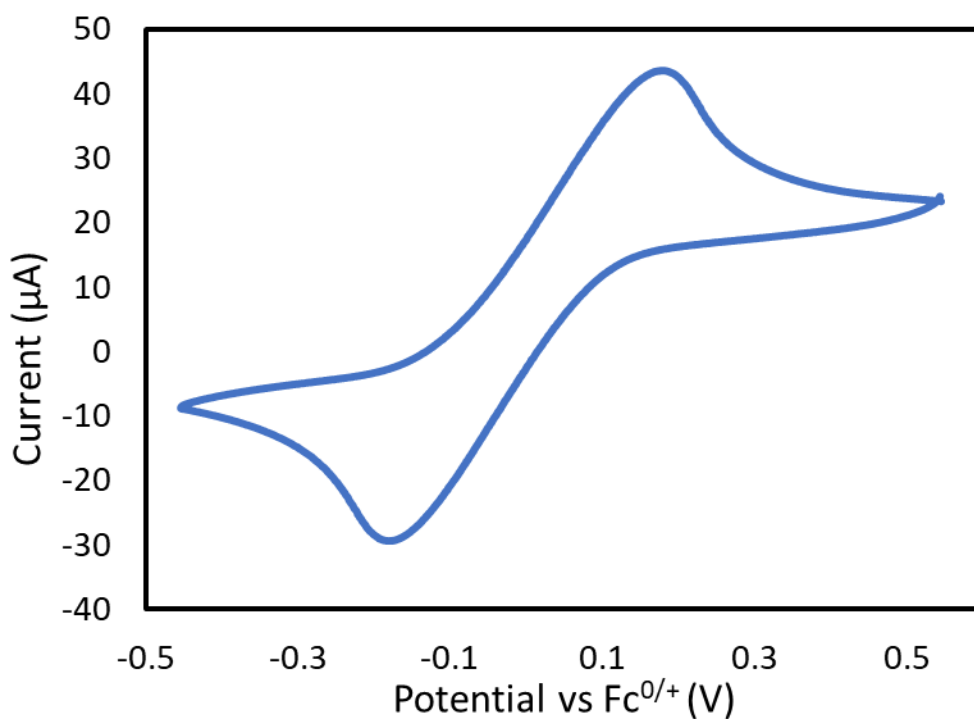


Figure S4: CV of 0.5mM Ferrocene in DCM scanned between 0.45V and -0.5V with a scan rate of 0.1V/s and electrolyte (TBAHFP) concentration of 0.1M.

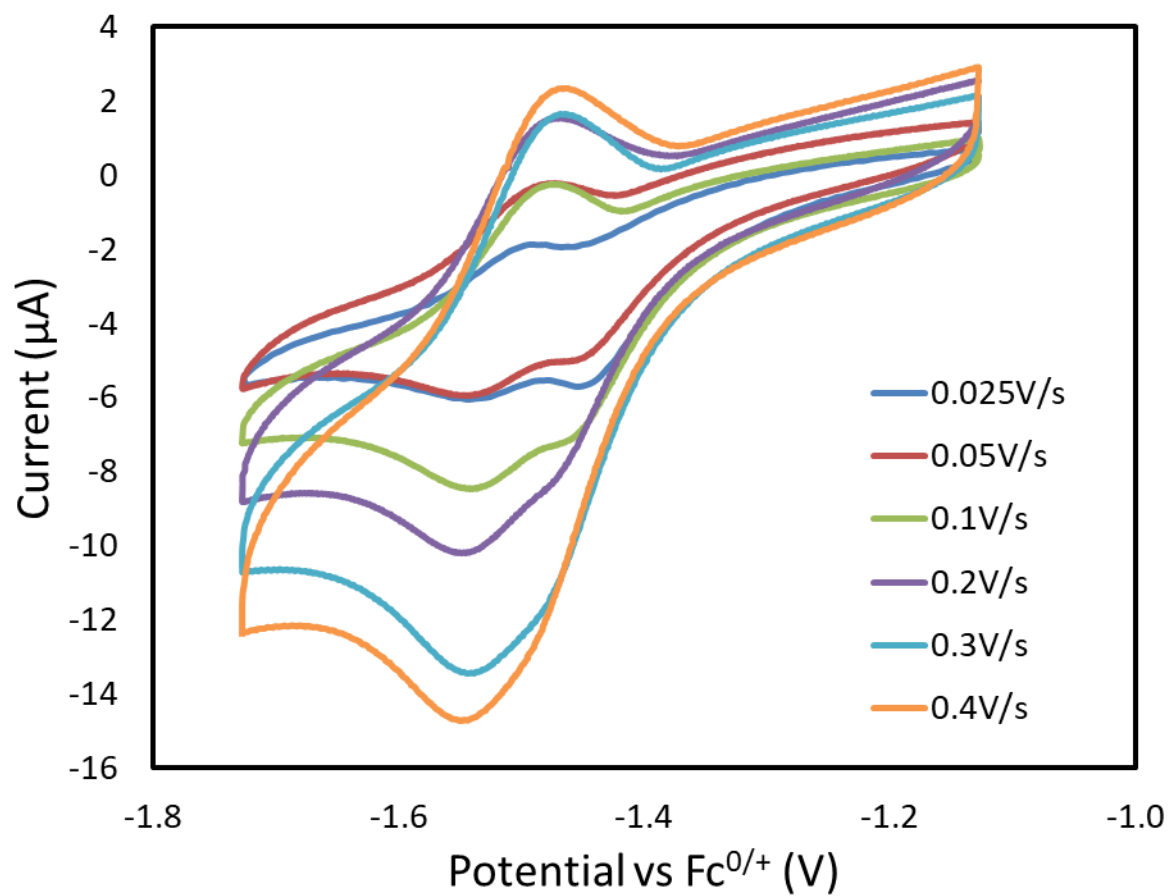


Figure S5: CV of 0.5mM **NiPc** in THF with a water concentration of 9.25M scanned between -1.15V and -1.75V with a varying scan rate and electrolyte (TBAHFP) concentration of 0.1M

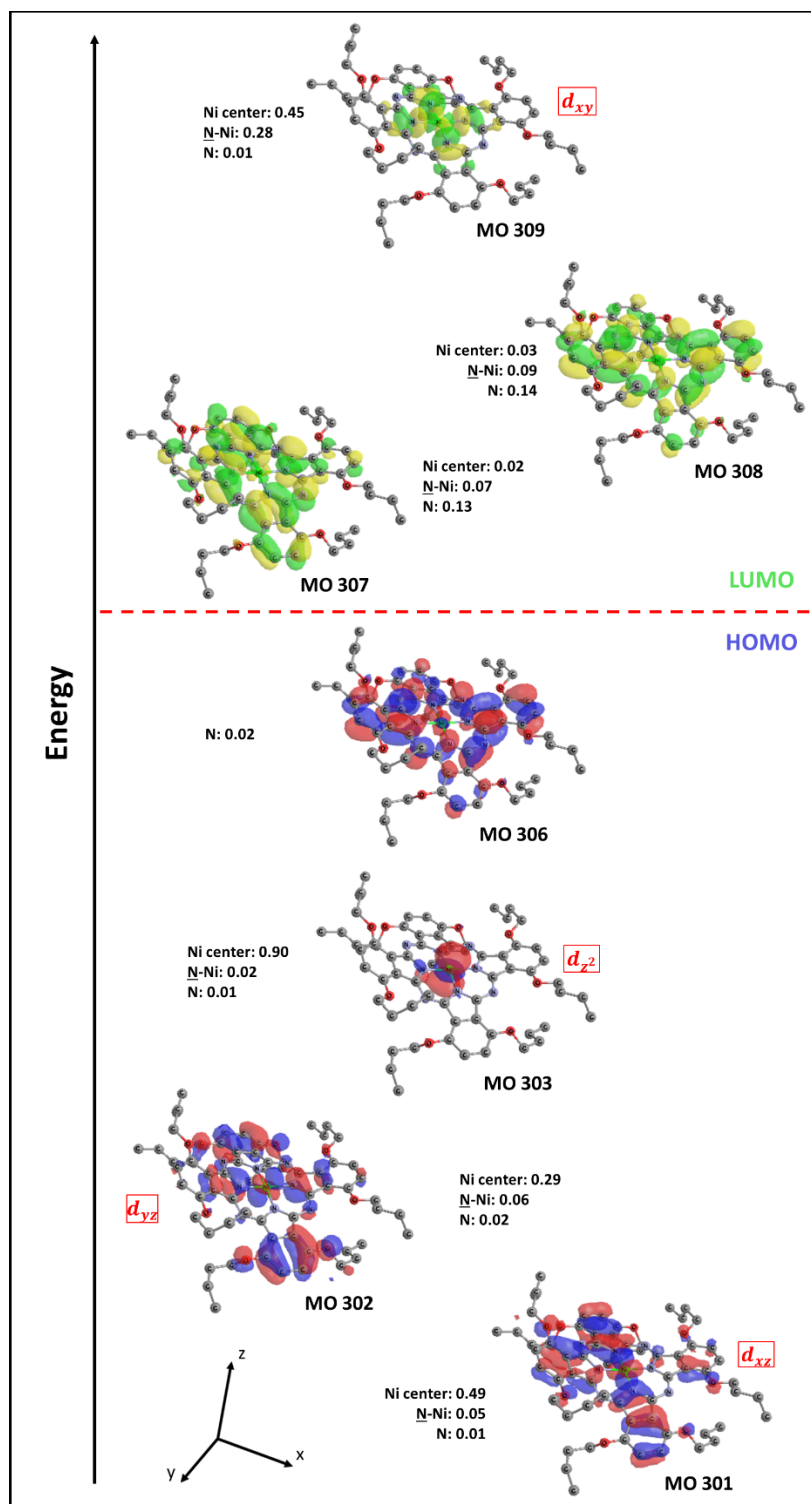


Figure S6: Selected molecular orbitals of **NiPc** in a singlet state computed at the M06L level of theory with def2-TZVP basis set.

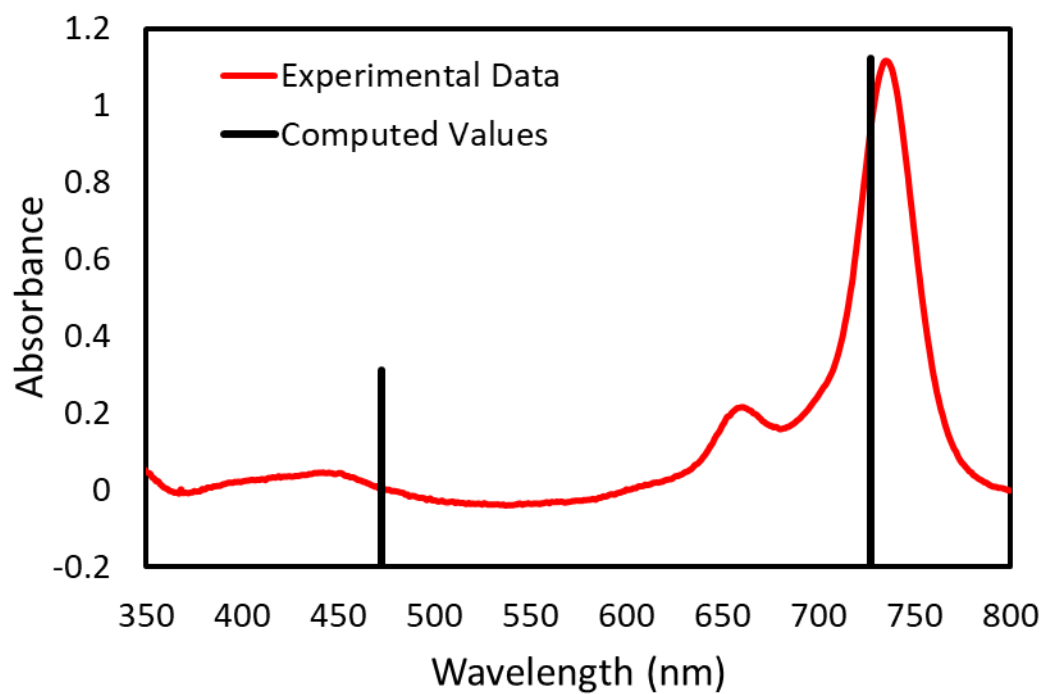


Figure S7: UV vis spectrum (red curve) of 0.017mM **NiPc** in DCM scanned between 800nm and 350nm. Computed values (TD-DFT) for electronic transitions of **NiPc** at the B3LYP level of theory with def2-TZVP basis set are shown as black lines.

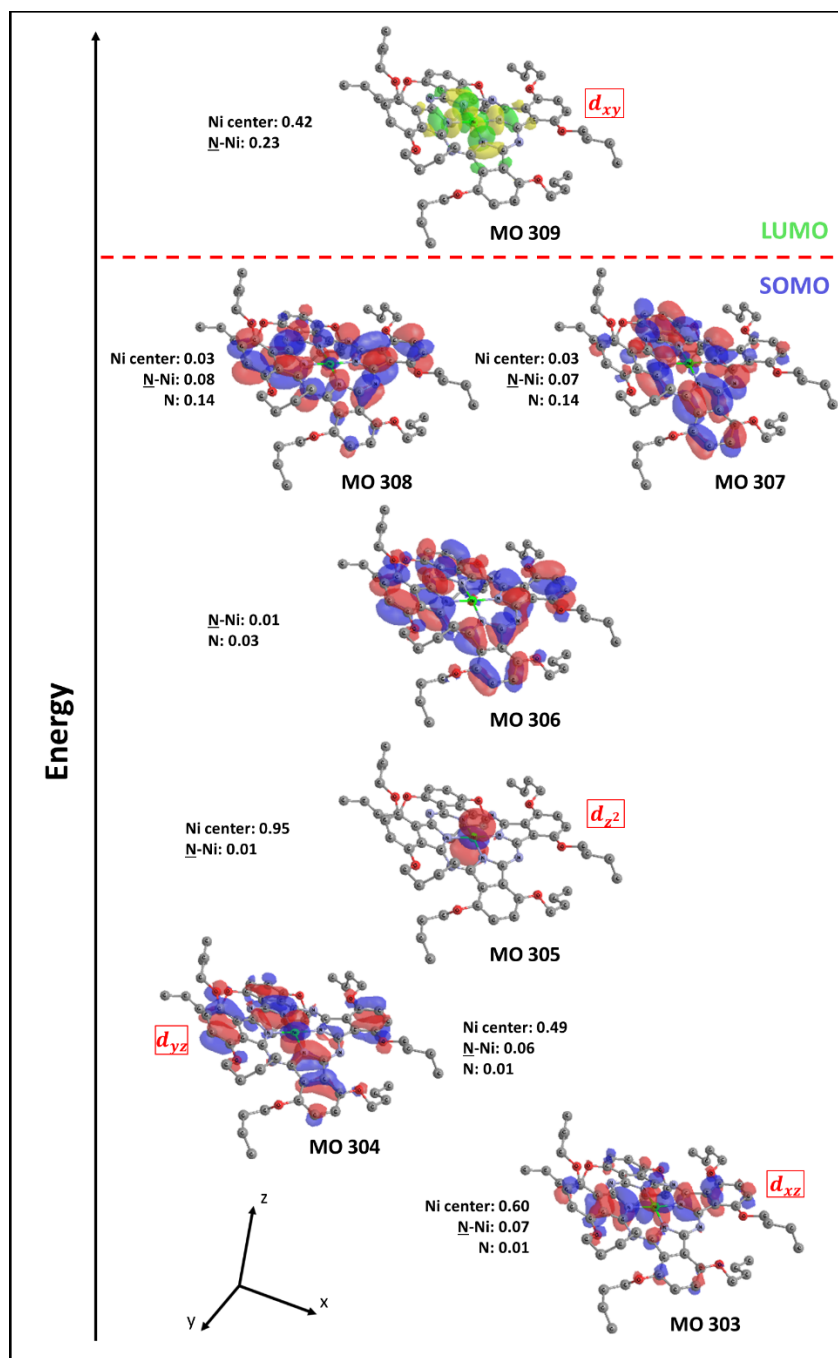


Figure S8: Selected molecular orbitals of NiPc^{2-} in a triplet state computed at the M06L level of theory with def2-TZVP basis set.

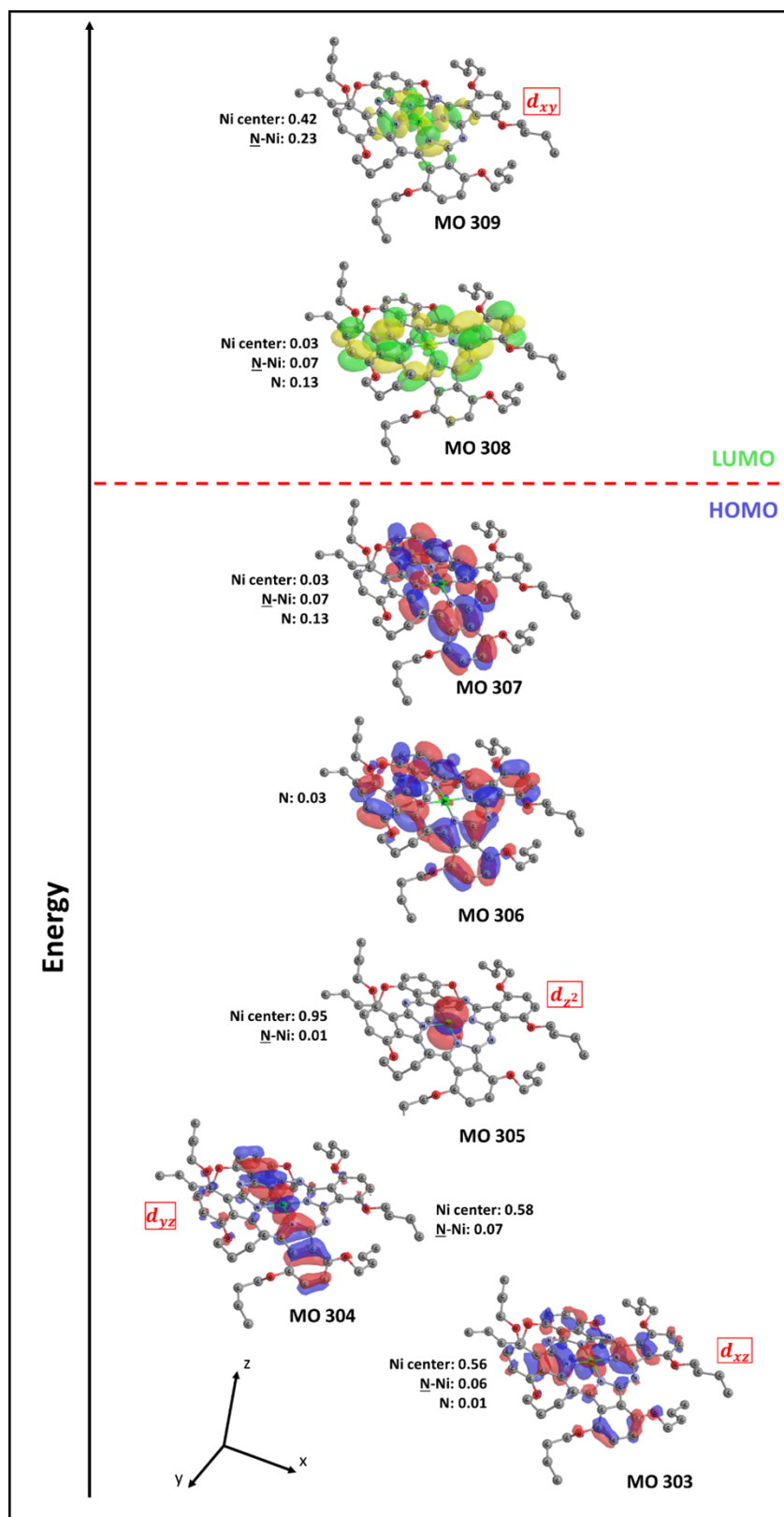


Figure S9: Selected molecular orbitals of NiPc^{2-} in a singlet state computed at the M06L level of theory with def2-TZVP basis set.

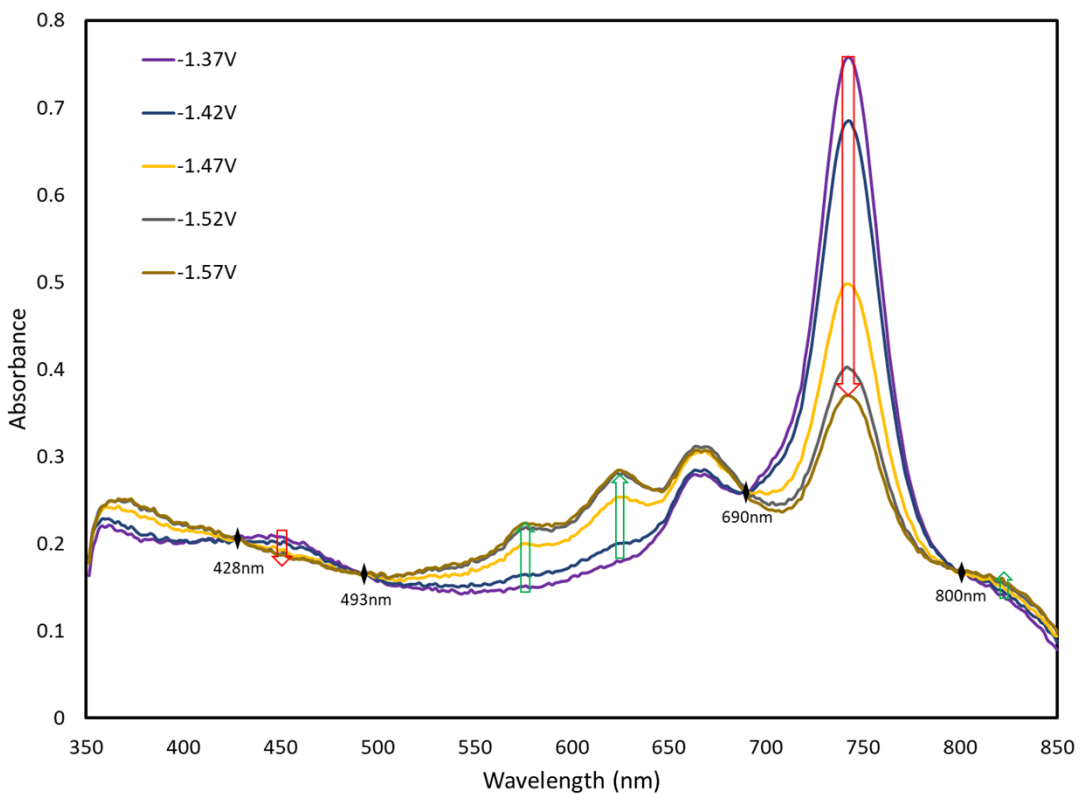


Figure S10: UV-vis spectra of 0.017mM **NiPc** in DCM. Multiple spectra were collected with an applied potential, starting at -1.12V and stepping by 0.05V until -1.62V vs $\text{Fc}^{0/+}$. The isosbestic points at 428, 493, 690 and 800 nm are indicated. The increasing (green arrow) and decreasing (red arrow) absorbances are shown.

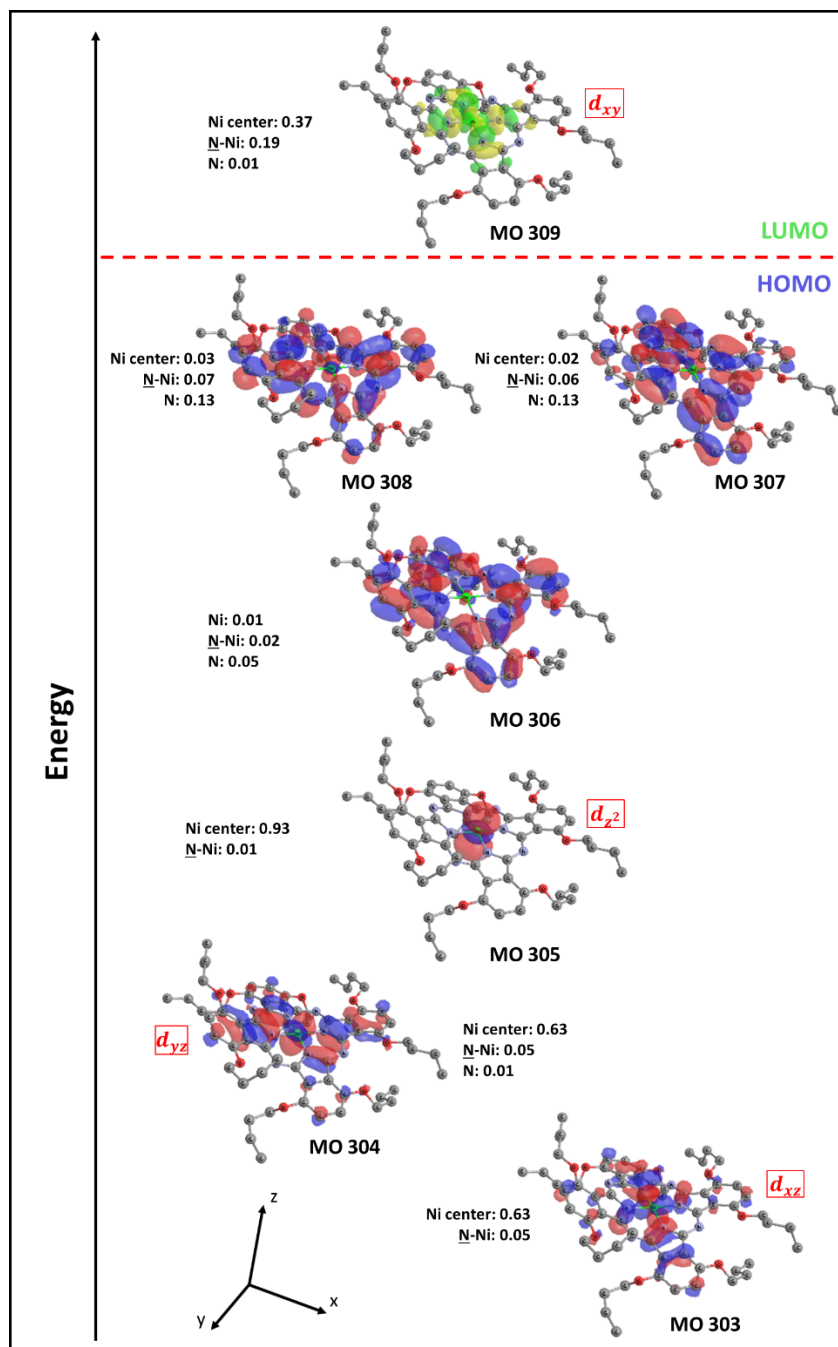


Figure S11: Selected molecular orbitals of **NiPc⁴⁺** in a singlet state computed at the M06L level of theory with def2-TZVP basis set.

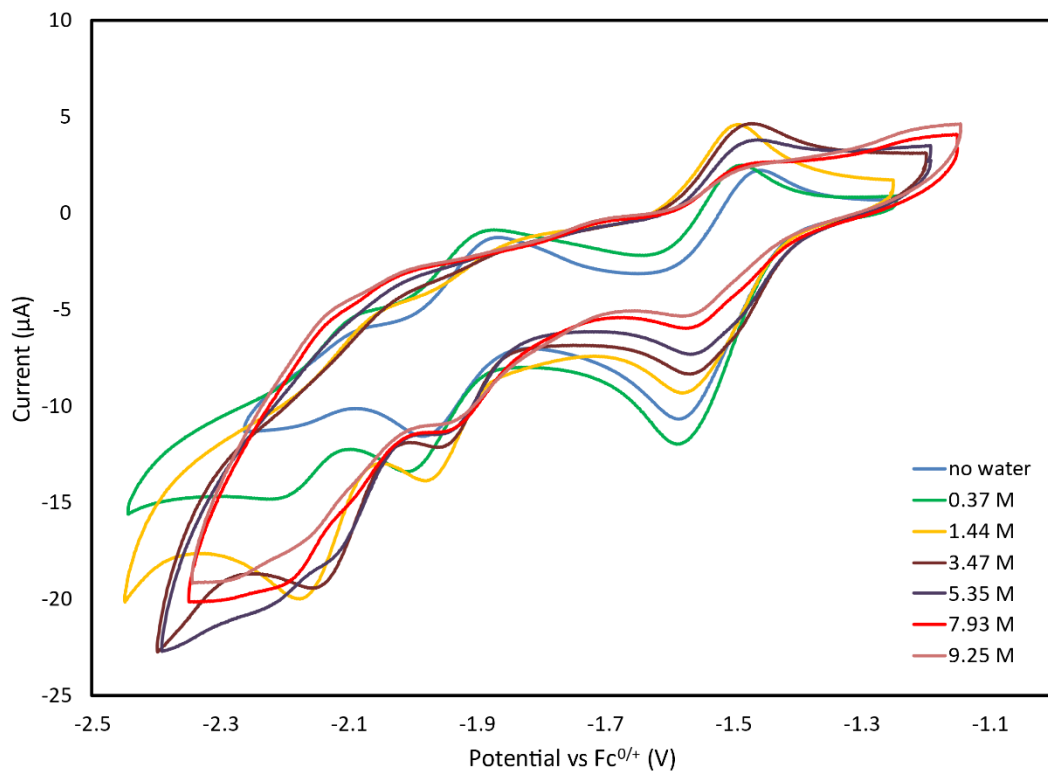


Figure S12: The effect of added water on the CV's of 0.5mM **NiPc** in THF with 0.1M electrolyte (TBAHFP). The CV's was scanned between -1.1V and -2.45V with increased water concentration as shown in the legend.

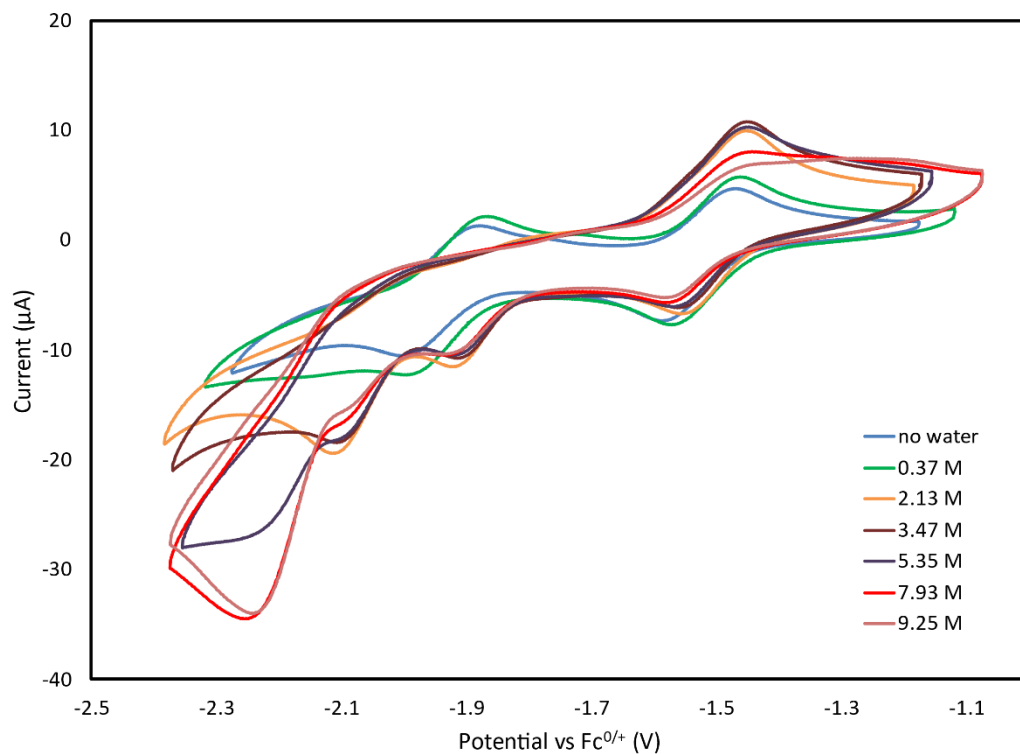


Figure S13: The effect of added water on the CV's of 0.5mM **NiPc** in THF with 0.1M electrolyte (TBAHFP) and 0.05M TEA. The CV was scanned between -1.1V and -2.45V with increased water concentration as shown in the legend.

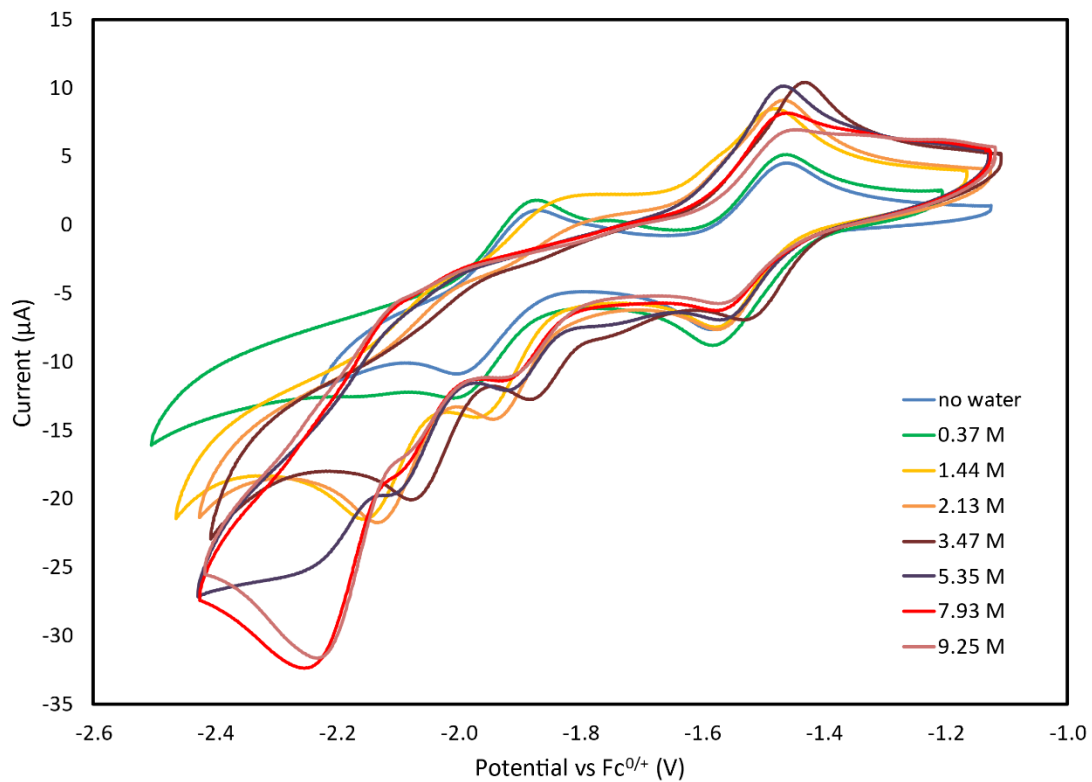


Figure S14: The effects of added water on CV's of 0.5mM **NiPc** in THF with 0.1M electrolyte (TBAHFP) and 0.2M TEA. The CV was scanned between -1.1V and -2.45V with increased water concentration as shown in the legend.

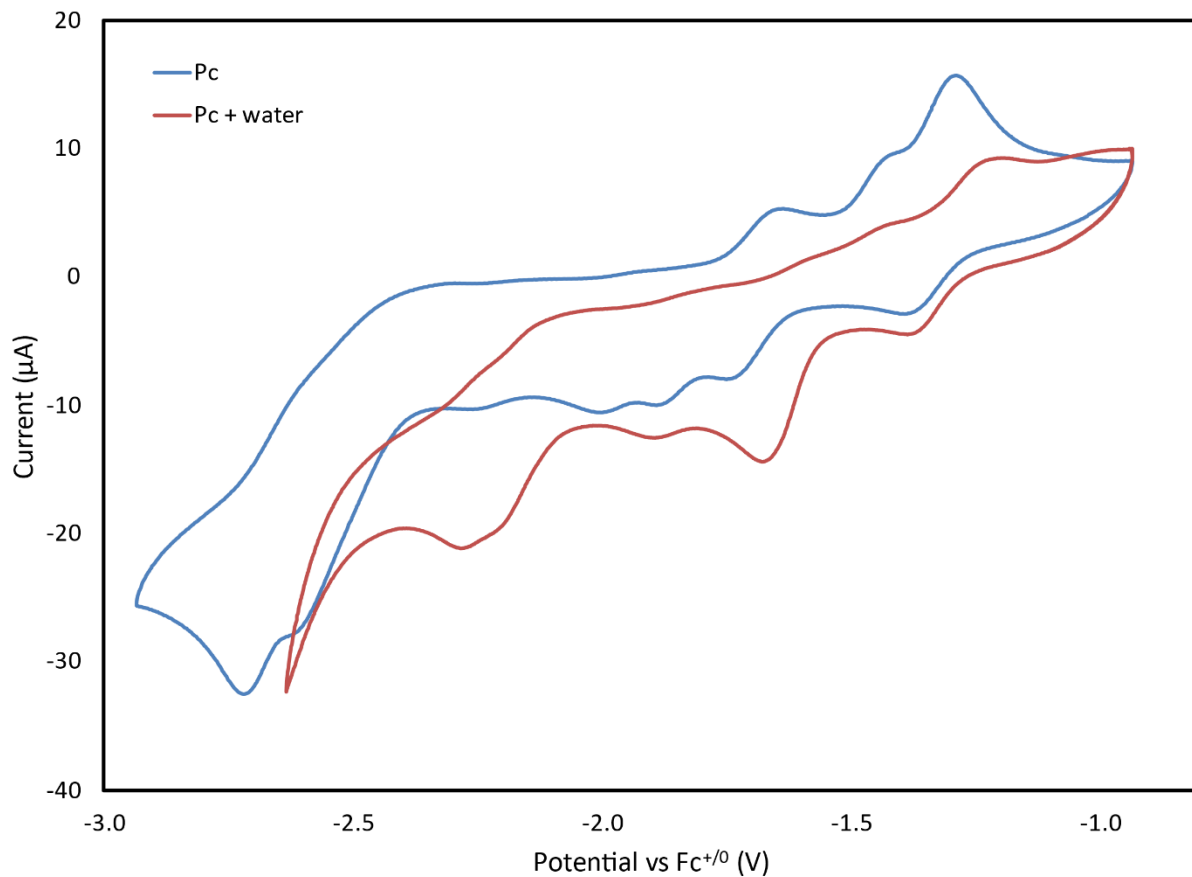


Figure S15: CV of 0.5mM free **Pc** ligand in THF scanned between -1.1V and -2.9V (blue curve). The red curve shows the same sample with added [H₂O] of 9.25M scanned from -1.1V to -2.6V.

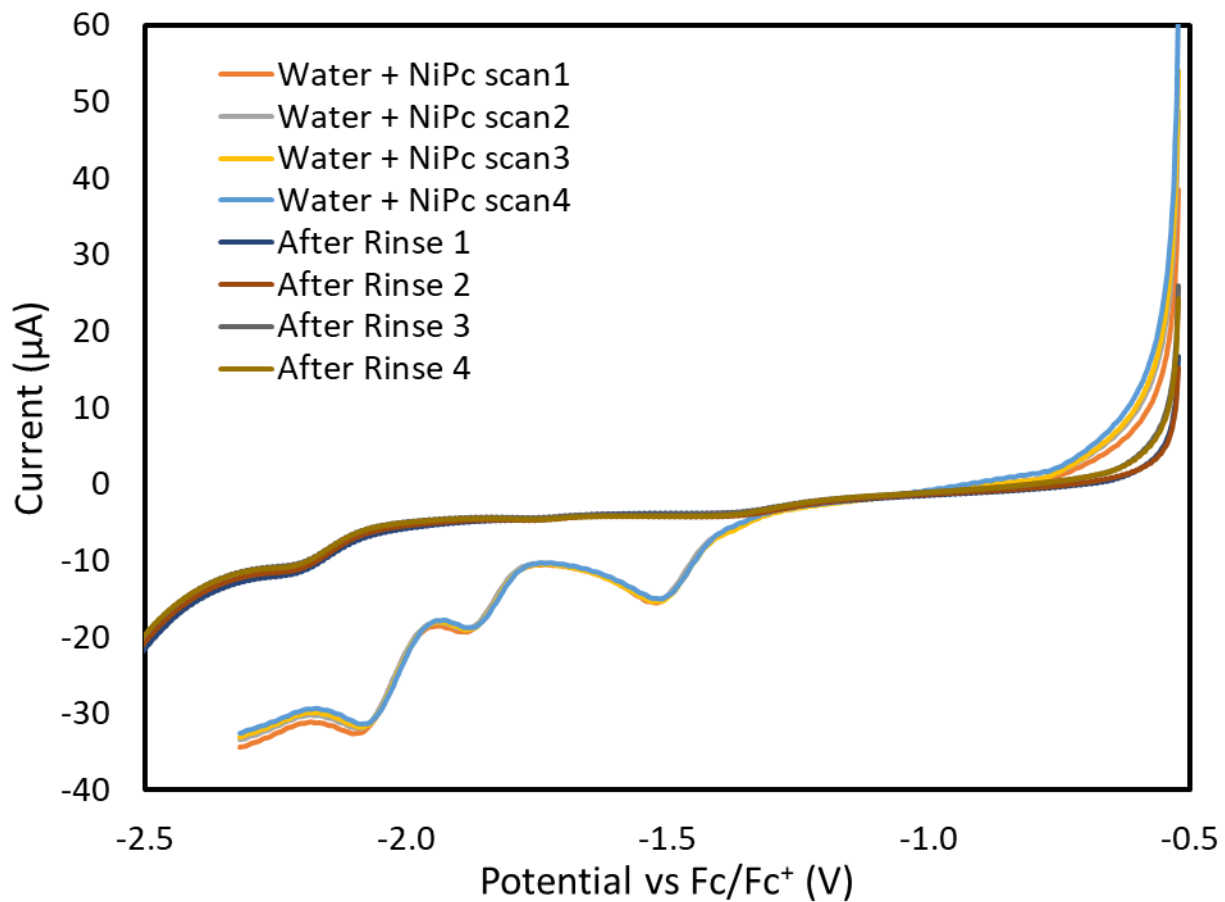


Figure S16: Linear sweep voltammograms of 0.5mM **NiPc** in THF with a water concentration of 6.53M before and after solvent rinse. Scans performed from -0.5V to -2.3V volts before rinse and -0.5V to -2.5V after rinse.

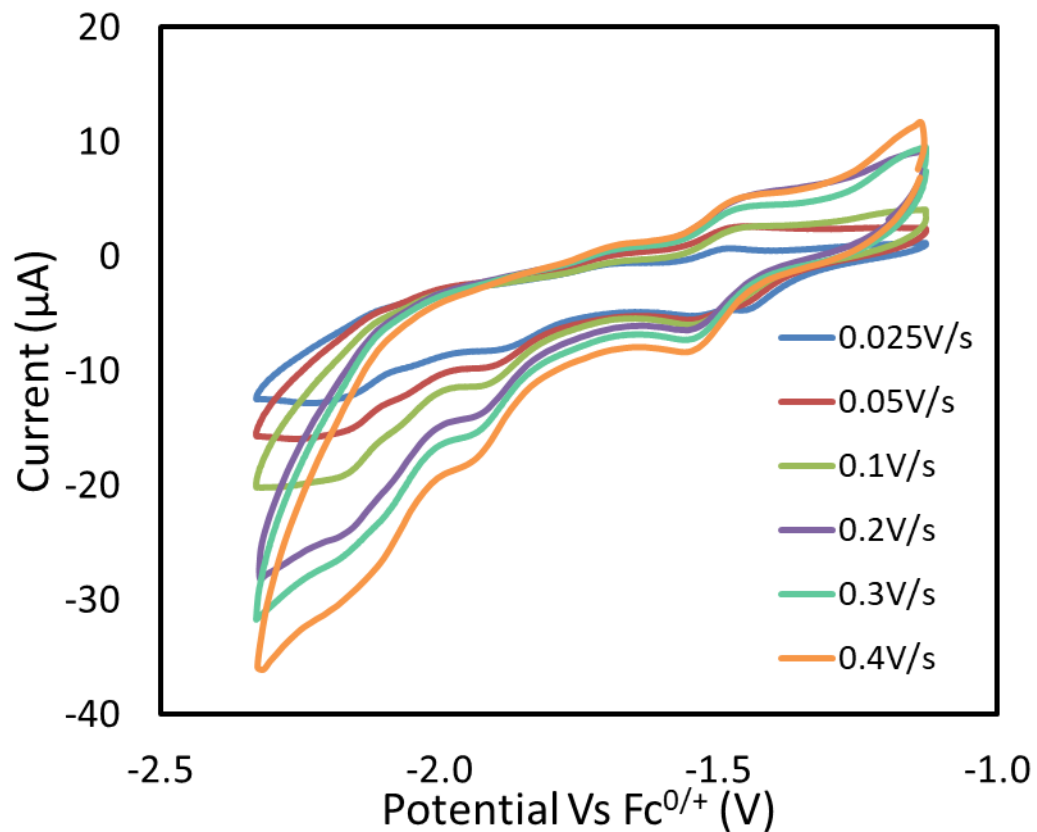


Figure S17: CV of 0.5mM **NiPc** in THF scanned between -1.15V and -2.35V with a varying scan rate and electrolyte (TBAHFP) concentration of 0.1M and water concentration of 9.25M.

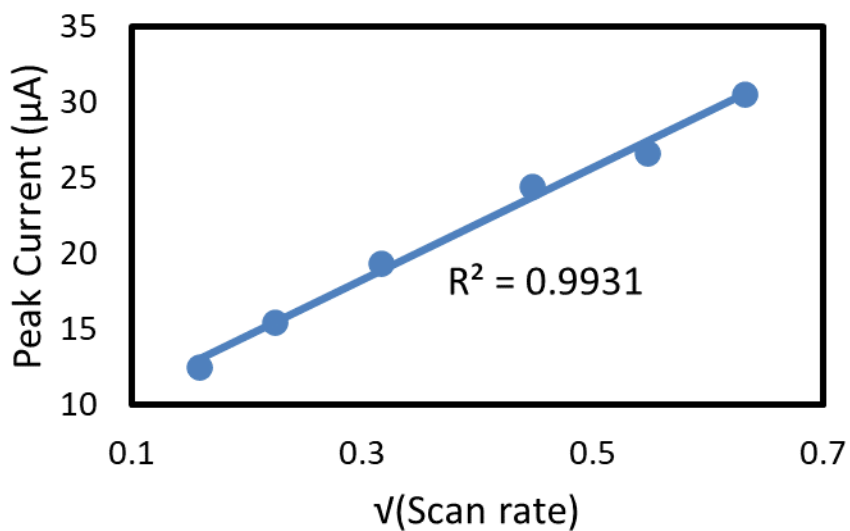


Figure S18: Plot of the reduction peak current value from figure S17 as a function of the square root of the scan rate at the catalytic redox event (-2.1V vs $\text{Fc}/\text{Fc}^{+/0}$)

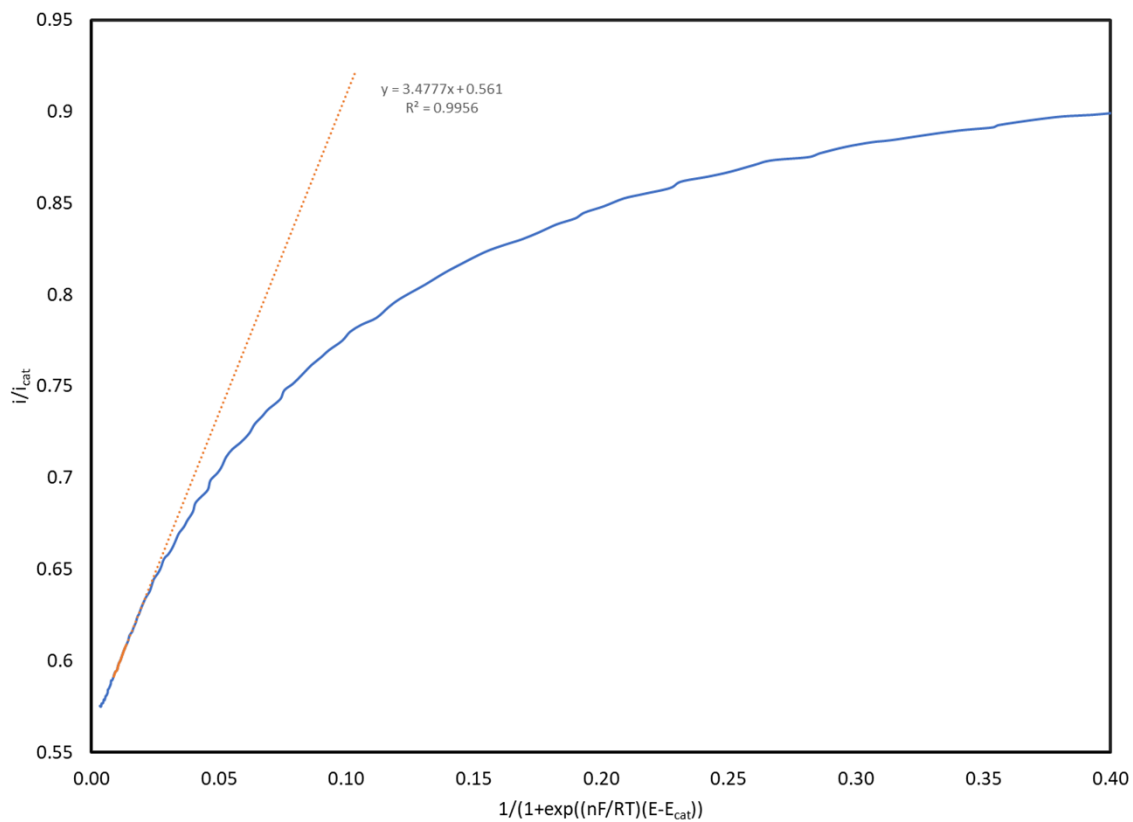


Figure S19: FOWA for **NiPc** with no added TEA. The orange line represents the slope, given by $2.24V RT(TOF) n'Fv$ with $n' = 2$ for the reduction of water to H_2 . The equation for the line is given in the figure.

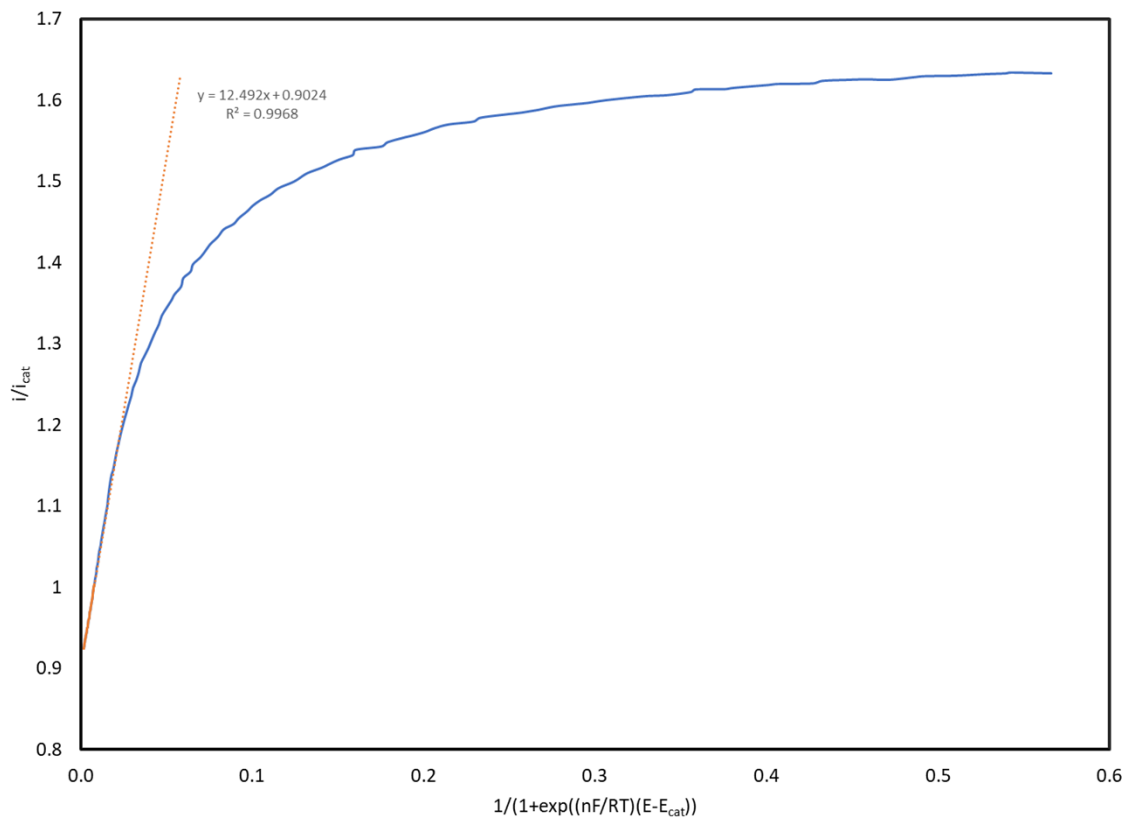


Figure S20: FOWA for **NiPc** with a TEA concentration of 0.05M. The orange line represents the slope, given by $2.24V RT(TOF) n'Fv$ with $n' = 2$ for the reduction of water to H_2 . The equation for the line is given in the figure.

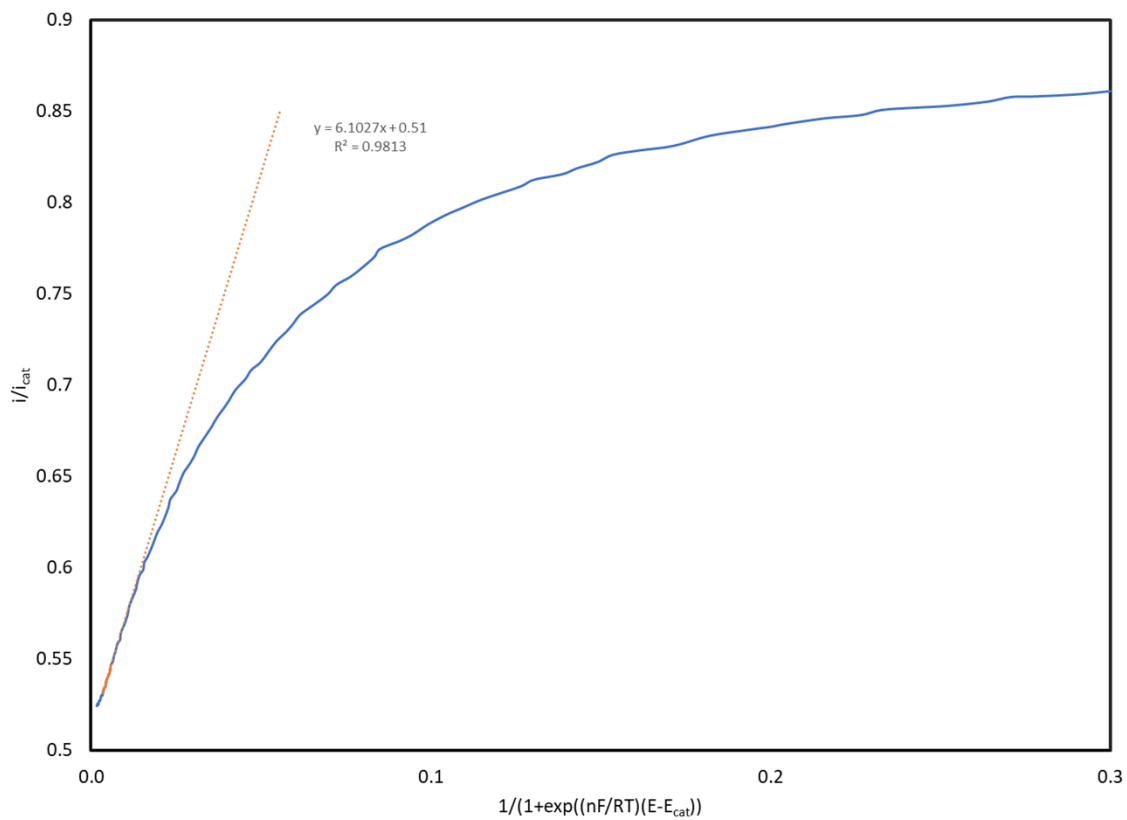


Figure S21: FOWA for **NiPc** with a TEA concentration of 0.2M. The orange line represents the slope, given by $2.24V RT(TOF) n'Fv$ with $n' = 2$ for the reduction of water to H_2 . The equation for the line is given in the figure.

Table S1: Results for Bulk 2-hour electrolysis Experiments performed at -2.15V vs $\text{Fc}^{+/0}$

Trial [TEA]	Electrons Passed (mol)	H_2 generated (mol)	FE*
0M	17.29	6.01	69%
0.05M	37.73	13.61	72%
0.2M	17.84	7.92	89%

*FE was calculated by dividing the total moles of H_2 produced (quantified by GC-TCD) by the theoretical H_2 . Theoretical H_2 was derived from the total charge collected in the bulk electrolysis and then corrected by subtracting 3 electrons associated with priming NiPc that are not involved in the catalysis.

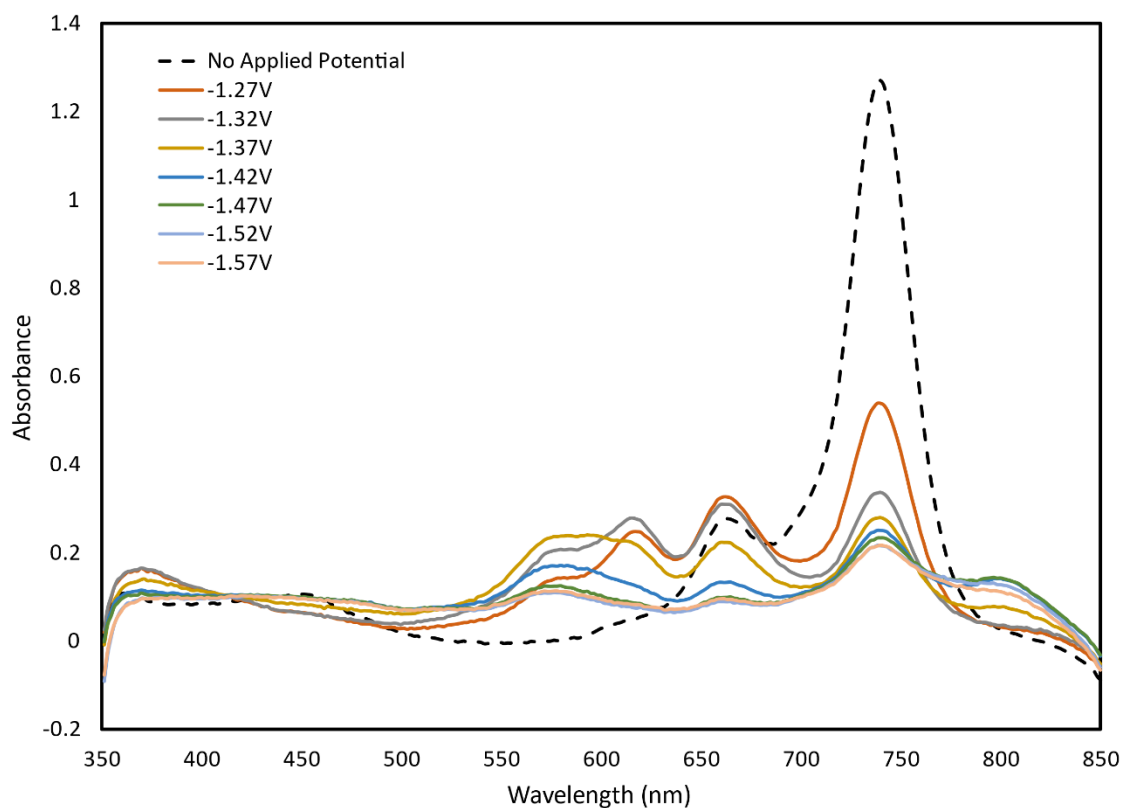


Figure S22: UV-vis spectra of 0.017mM **NiPc** in THF with a water concentration of 9.25M. Multiple spectra were collected with an applied potential, starting at -1.27V and stepping by 0.05V until -1.57V vs $\text{Fc}^{0/+}$.

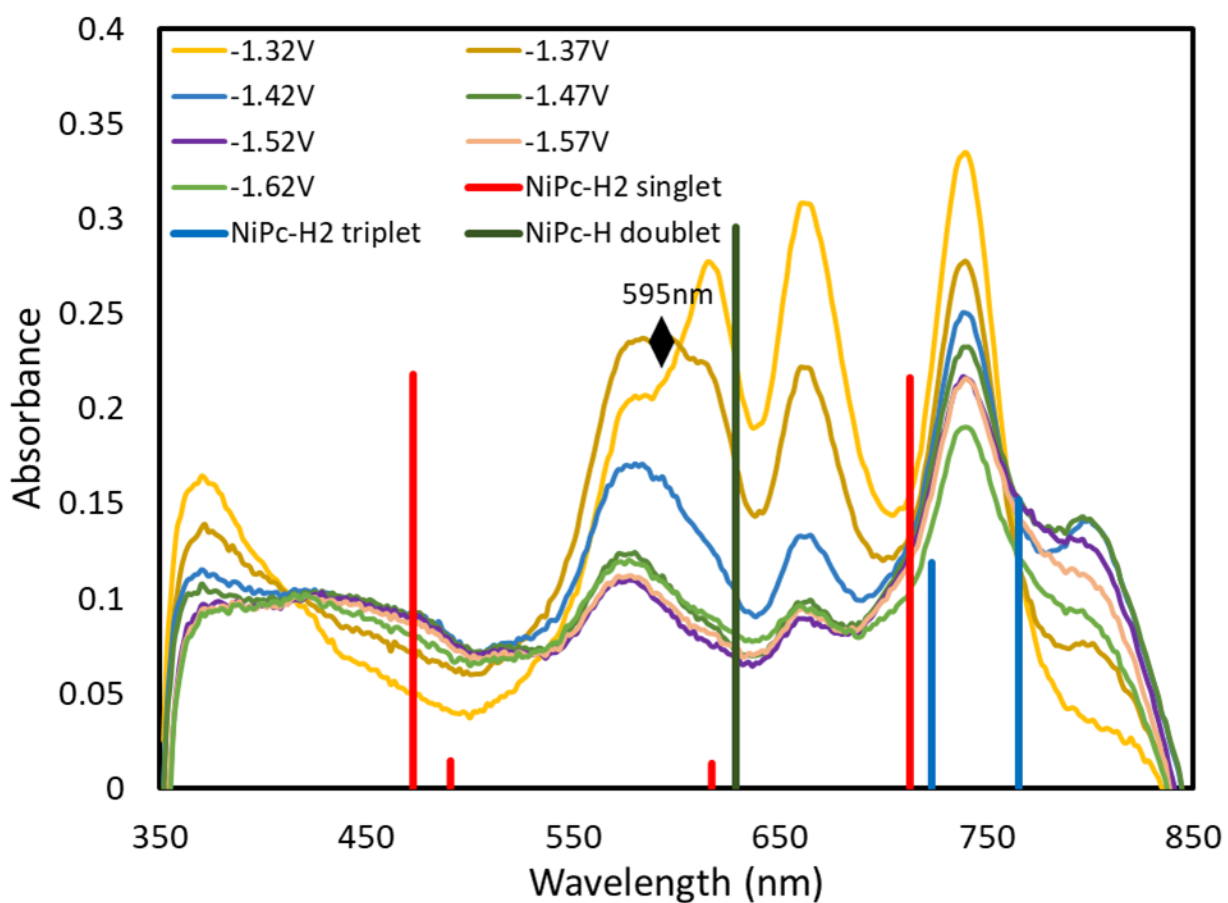


Figure S23: UV-vis spectra of 0.017mM **NiPc** in THF with a water concentration of 9.25M. Multiple spectra were collected with an applied potential, starting at -1.32V and stepping by 0.05V until -1.62V vs $\text{Fc}^{0/+}$. DFT simulation of the singlet and triplet states for **NiPc-H₂** and **NiPc-H** doublet are included at the B3LYP level of theory and def2-TZVP basis set.

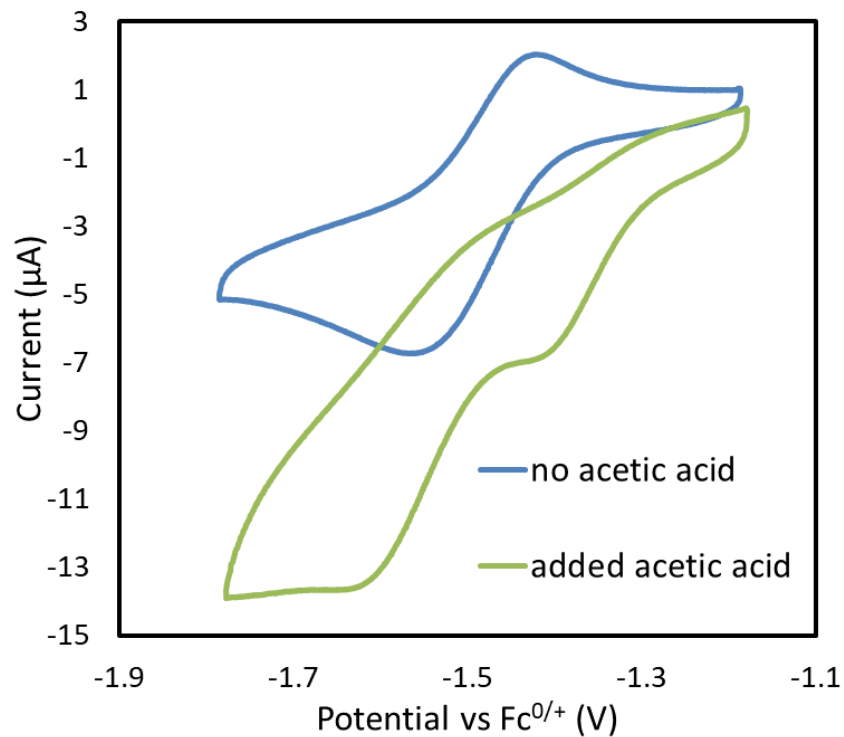


Figure S24: CV of 0.5mM **NiPc** in DCM scanned between -1.18V and -1.77V (blue curve). A similar CV with an added acetic acid concentration of 0.13M (green curve).

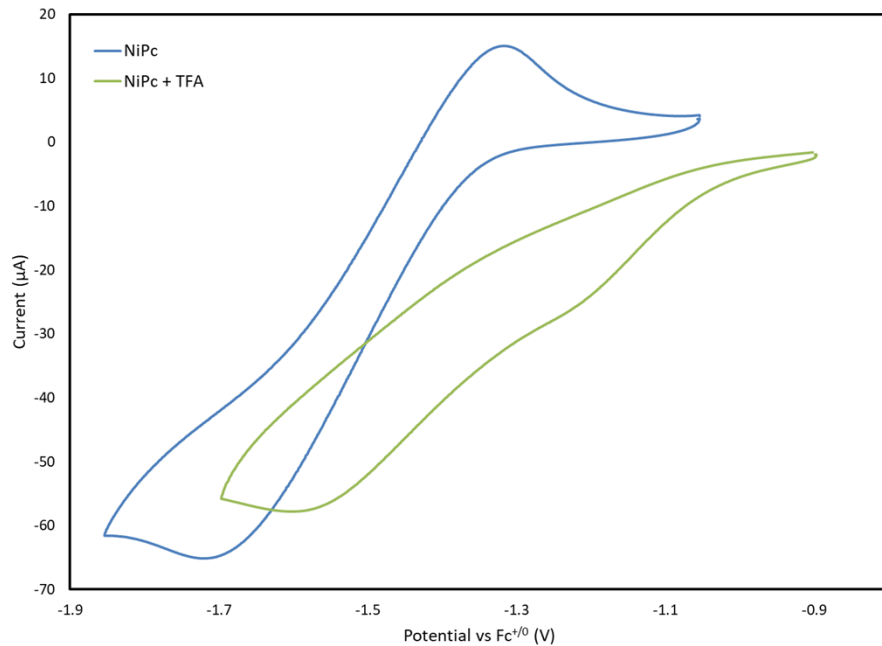


Figure S25: CV of 0.5mM **NiPc** in THF (blue curve) and a similar CV with an added trifluoroacetic acid (TFA) at 20mM concentration (green curve).

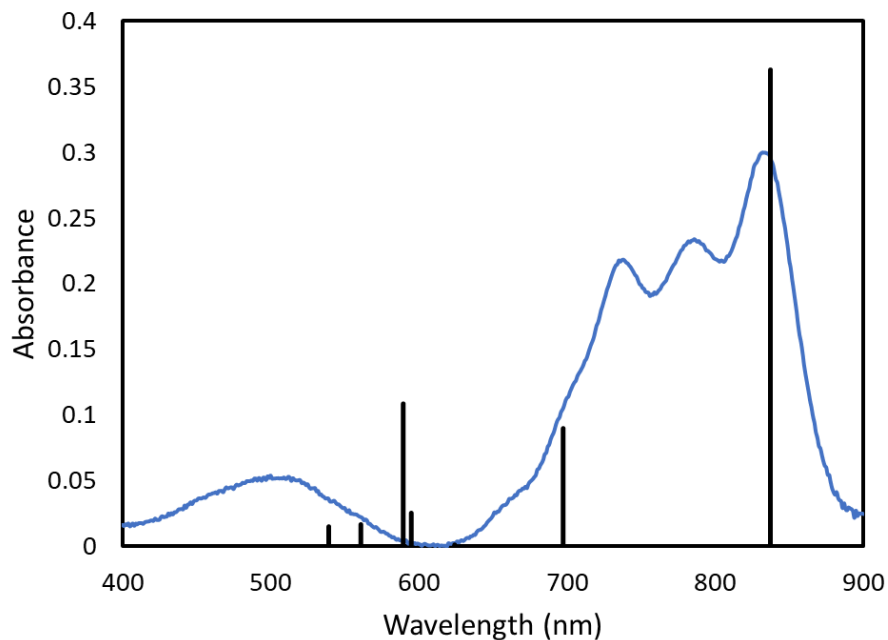


Figure S26: Absorbance spectrum of 0.017mM **NiPc** in DCM scanned between 800nm and 400nm with addition of 1eq of TFA. The TD-DFT computed values for the electronic transitions of **NiPc-H⁺** at the B3LYP level of theory with def2-TZVP basis set are shown as black lines at 838, 687, and 589nm.

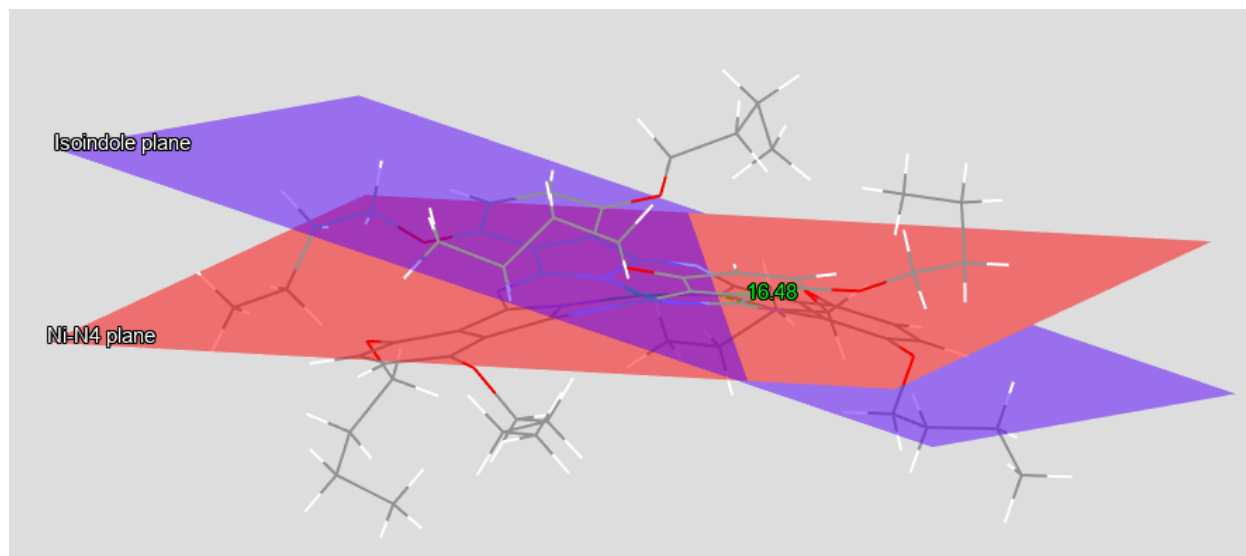


Figure S27: Wire plot of **NiPc** computed with the M06L functional with the def2-SVP basis set. The Isoindole plane is defined as the planar surface that contains all atoms in the selected isoindole group. The Ni-N4 plane intersects with the Isoindole plane at the coordinated nitrogen atom containing the four coordinated nitrogen and the nickel metal center.

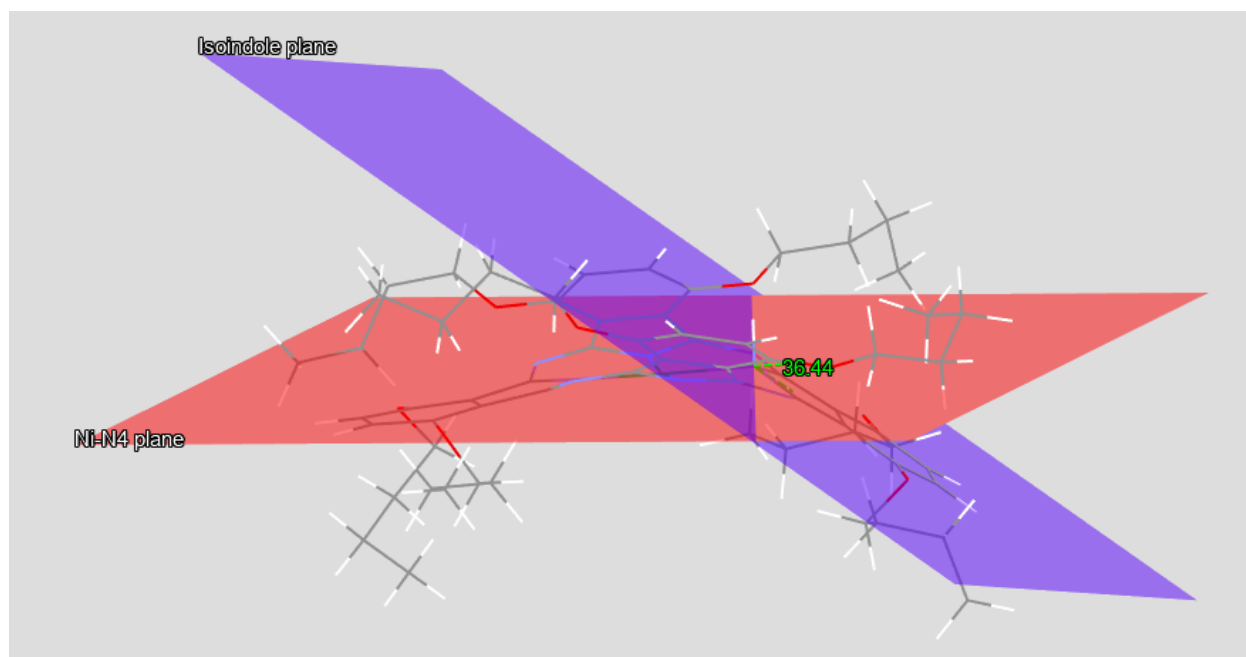


Figure S28: Wire plot of **NiPc** protonated on a coor-N center (**NiPc-H⁺**) simulation computed with the M06L functional with the def2-SVP basis set. The Isoindole plane and Ni-N4 plane are defined in the same way as figure 26, centered at the protonated Coor-N.

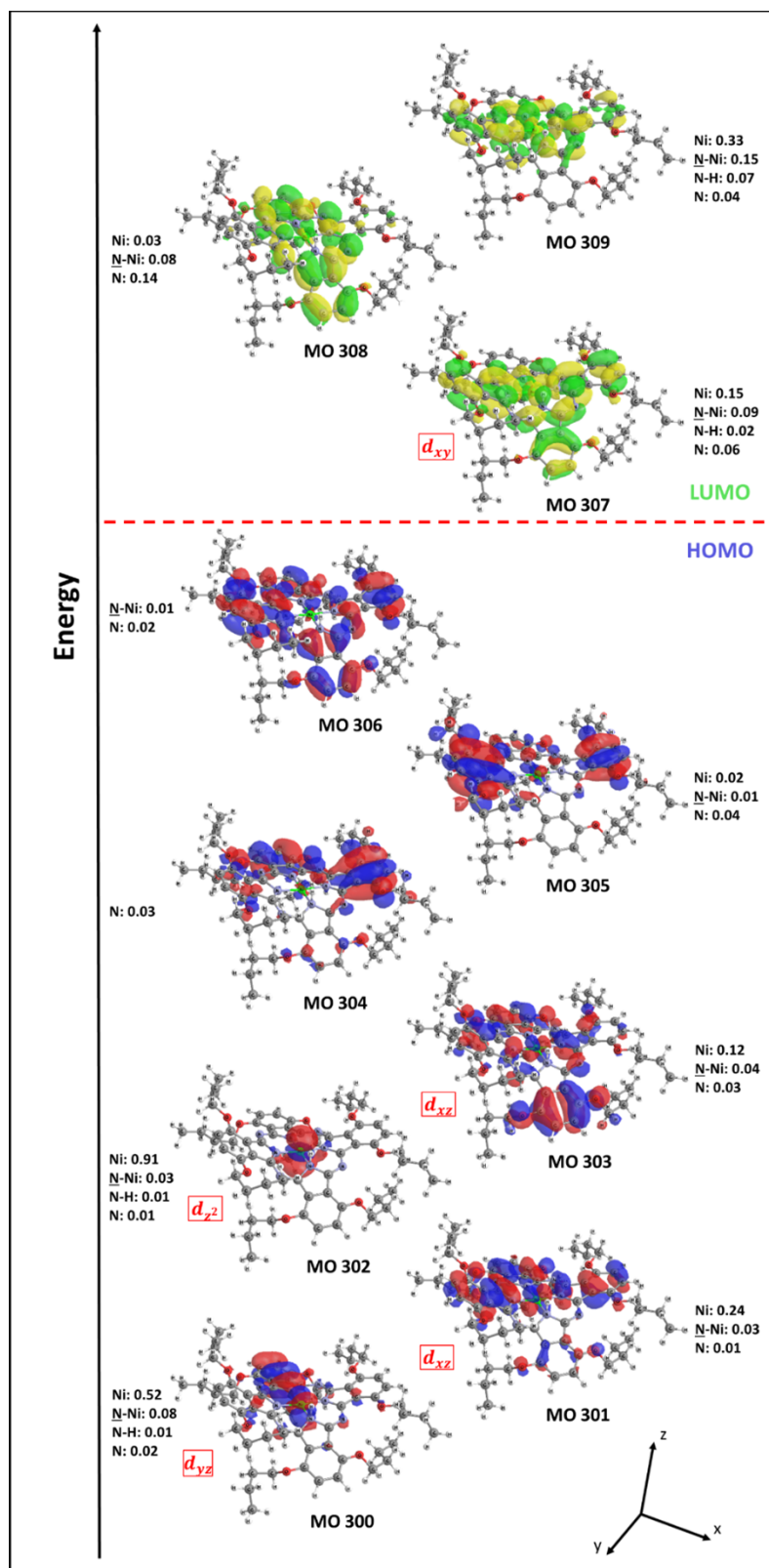


Figure S29: Selected molecular orbitals of **NiPc-H⁺** in a doublet state computed at the M06L level of theory with def2-TZVP basis set.

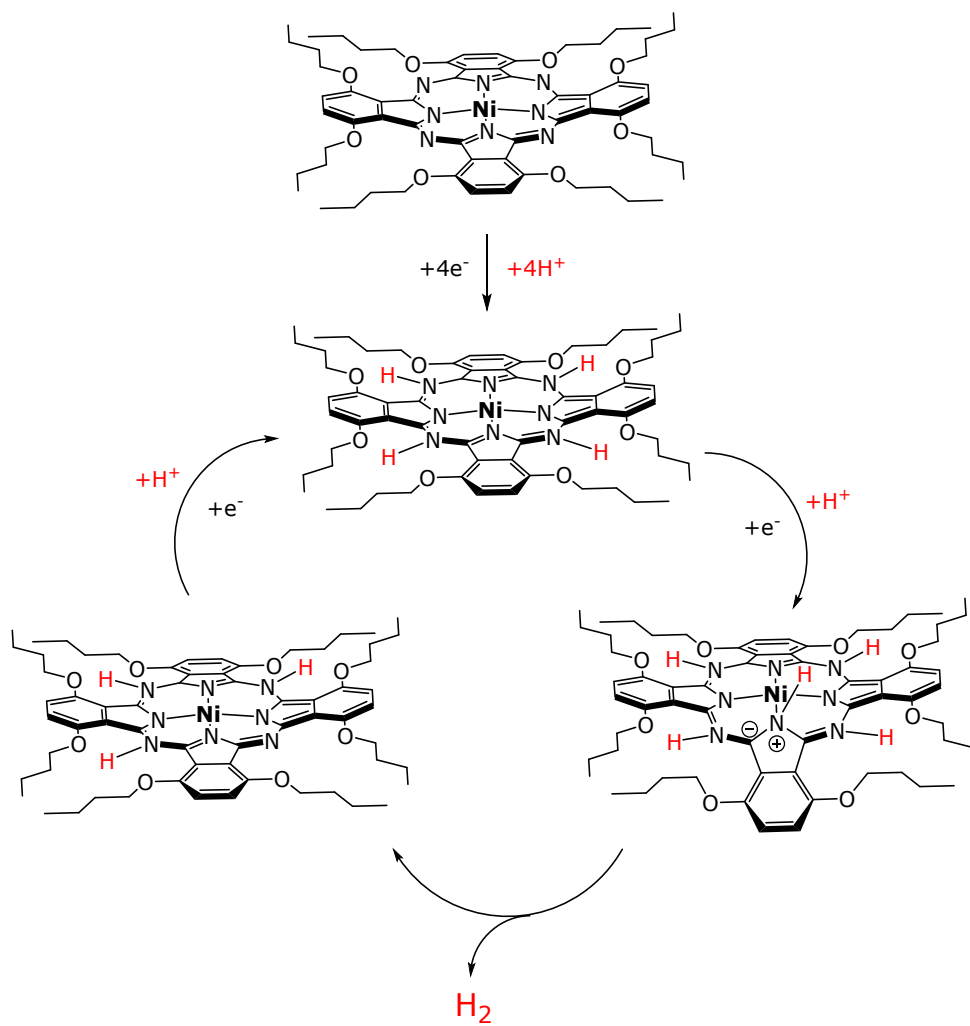


Figure S30. Chemdraw representation for a proposed mechanism for H₂ generation from NiPc.

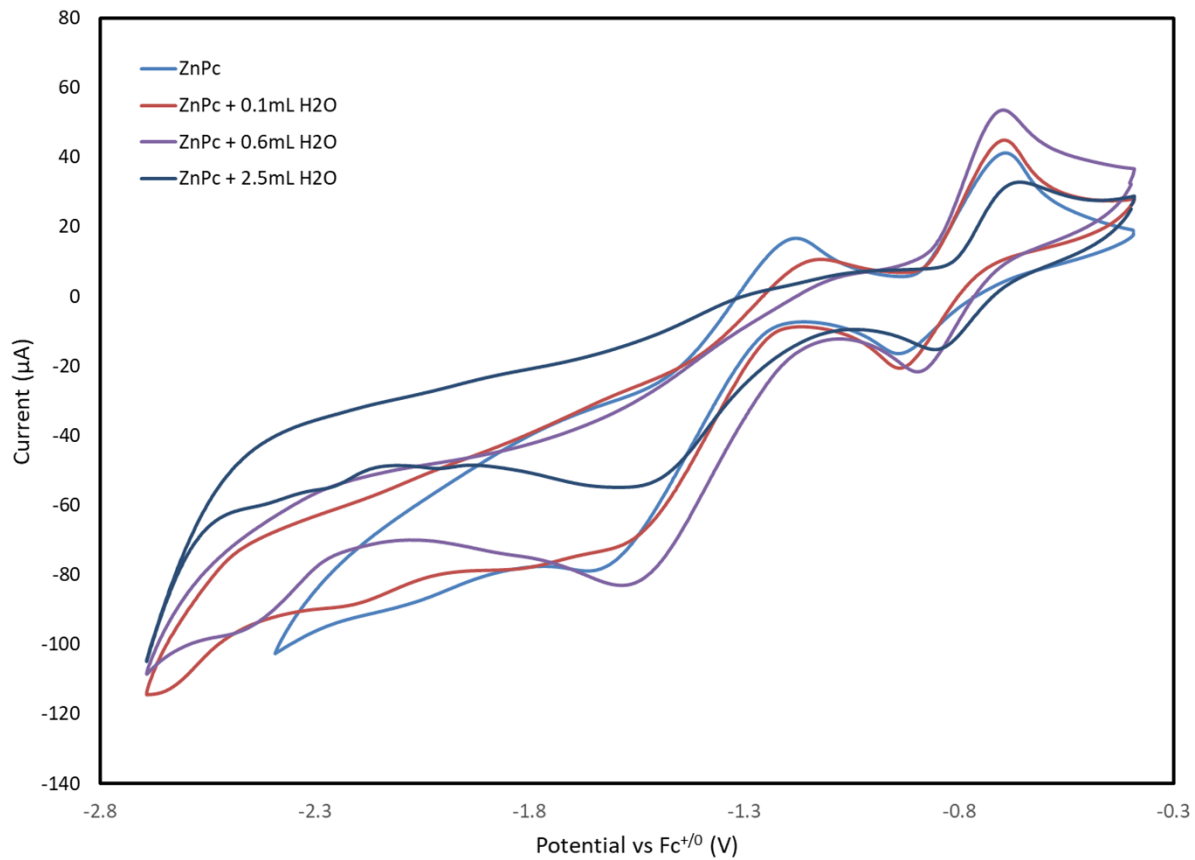


Figure S31: The effect of added water on the CV's of 0.5mM **ZnPc** in THF with 0.1M electrolyte (TBAHFP) and 0.05M TEA. The CV's were scanned between -0.4V and -2.7V with additions of water, as shown in the legend.